Drop spreading on heterogeneous substrates via Monte Carlo simulations

Nina Pesheva*
Institute of Mechanics, Bulgarian Academy of Sciences, Academician G. Bonchev Street 4, 1113 Sofia, Bulgaria

Joël De Coninck†
Centre de Recherche en Modélisation Moléculaire, Université de Mons-Hainaut, Parc Initialis-Avenue Copernic, Bât. Materia Nova-7000 Mons, Belgium

(Received 26 March 2004; published 6 October 2004)

We study the dynamics of liquid drops in the partial wetting regime first on pure surfaces and then on heterogeneous substrates. We model the spreading of a drop by a 3-dimensional Ising model (3D IM). The initial nonequilibrium configuration is a parallelepiped of occupied sites with appropriately chosen boundary conditions from which we let the system evolve towards its equilibrium state via a particle-conserving dynamics. We find that the time behaviors of the base radius $R_1(t)$ and the cosine of the contact angle $\cos\theta(t)$ are well described by exponential decay functions with relaxation times τ_r and $\tau_{\cos\theta}$ correspondingly. Thus it follows that the molecular kinetic theory gives a valid description of the initial stage of drop spreading in the partial wetting regime for times smaller than both relaxation times τ_r and $\tau_{\cos\theta}$. Also, our MC results for the 3D IM with regularly distributed single-site impurities at low temperatures and low surface fields are compatible with Cassie's and Israelachvili's equations, the description of the data with Israelachvili's equation being slightly better. At high temperatures and high surface fields there is a deviation from the purely linear behavior of the cosine of the contact angle on the concentration known as Cassie's law for chemically heterogeneous surfaces.

DOI: 10.1103/PhysRevE.70.046102 PACS number(s): 05.50.+q, 05.10.Ln, 68.03.Hj

I. INTRODUCTION

The phenomena of spreading and wetting have many diverse applications in a wide number of processes and products in industry, which explains partly the new revived interest in the past decade. On the other hand, the development of new technologies has inspired new research. Due to the wide availability of computers, Monte Carlo algorithms have proved nowadays to be a powerful tool (for a review see e.g., [1]) to study the properties of many-particles systems, in that number simple fluids.

Simple models in physics have always played an important role in helping to improve the understanding of the microscopic origins of macroscopic behavior. The Ising model is a prototype model for many studies in statistical physics. Monte Carlo simulations of IM have been used to study the dynamics of liquid droplet spreading in $D=2$ dimensions [2] yielding a linear growth with time of the width of the drop. Previous studies also include simulations of a variant of the 3D lattice gas (LG) with Lennard-Jones interaction potential in the partial wetting regime [3]. A 3D IM with conserving dynamics has already been successfully applied in studies of spreading in the complete wetting regime [4,5,6] recovering a diffusive behavior of the base radius, $R_1 \propto \sqrt{t}$, in agreement with the experimental results [7,8,9] and molecular dynamic simulations [10].

Here we extend these works to study in detail the time evolution of a liquid drop, modeled by a 3D IM with conserving dynamics, in the partial wetting regime first on pure surfaces and then on heterogeneous substrates.

This paper is organized as follows. First we present the model and the initial and boundary conditions employed. Then we present our results at equilibrium on homogeneous and heterogeneous substrates. In the next section we present our findings for the dynamics of spreading in the partial wetting regime. The last section is devoted to our conclusions.

II. THE MODEL, INITIAL AND BOUNDARY CONDITIONS

We use the well known kinetic 3D Ising model with conserving dynamics [11,12] to model our system. It is convenient to introduce basic ideas and quantities with reference to the conventional Ising model, while keeping in mind that spin-up (+) and spin-down (−) states are readily mapped onto the liquid and vapor states of a LG. The model is defined in the standard way. We consider a simple cubic lattice Λ with linear size L and with every lattice site $i=(i_x,i_y,i_z)$, $i\in\Lambda$, we associate a variable σ_i which takes on two values $\{+1,-1\}$. The corresponding Hamiltonian is

$$H=-J\sum_{\langle ij\rangle\in\Lambda}\sigma_i\sigma_j-\sum_{i\in\partial\Lambda}h_i\sigma_i, \tag{1}$$

where $J(J>0)$ is a constant describing the attraction between two molecules of the fluid in this simplified description. As usually, $\langle ij\rangle$ means that nearest-neighbor interactions are only considered and h_i describes a surface field acting at the boundaries of the lattice $\partial\Lambda$.

Schematic representation of the system is shown in Fig. 1. The initial nonequlibrium configuration is a parallelepiped of sites with $\sigma_i=+1$. The parallelepiped sizes are equal to the

*Electronic address: nina@imbm.bas.bg
†Electronic address: joel@galileo.umh.ac.be

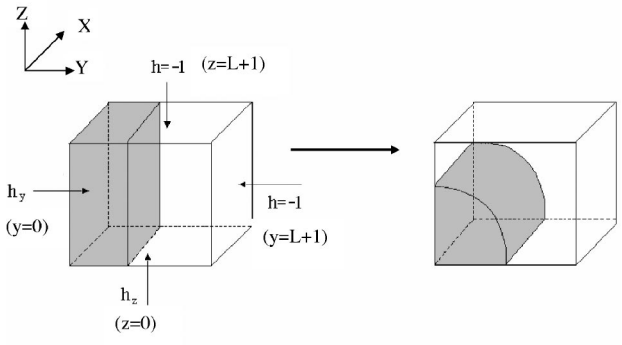

FIG. 1. Schematic representation of the model system in the initial state, the left cube, and in the final state, the right cube.

sizes of the system in the z and x directions, i.e., $l_x^p=L$, $l_z^p=L$, and l_y^p is chosen so that one gets a fixed density, i.e., $\rho=l_y^p/L$. The rest of the sites outside the parallelepiped are set to $\sigma_i=-1$.

In the x-direction periodic boundary conditions are imposed to reduce the finite-size effects. At the boundary planes, $z=L+1, y=L+1$, a field $h=-J$ is applied which favors the formation of a phase with a negative magnetization or a vapor phase in LG language. At the boundary plane $y=0$ a field $h_y=0.7J$ is imposed close to the bulk magnetization at the considered temperature, e.g., $m_b\approx 0.8$ at $T=3.8J/k_B$ [13] (see also Fig. 2) in order to model a half drop in a corner in the (z,y) plane. k_B is the Boltzmann constant.

In most cases, we also set the field h_z at the boundary plane $z=0$, modeling the interaction with the substrate, to be equal to h_y, i.e., $h_z=h_y$, to ensure better statistics.

We then let the system evolve towards its equilibrium state through a Kawasaki dynamics which preserves the total magnetization M_{tot} in the system. The following, Kawasaki rate function is used:

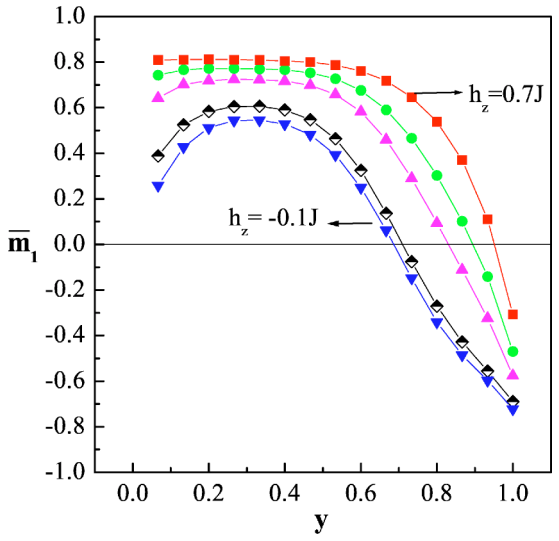

FIG. 2. (Color online) The averaged magnetization $\bar{m}_1$ of the first layer $(z=1)$ of the drop versus the scaled distance $y=Y/L$ at equilibrium $(T=3.8J/k_B, \rho=0.4)$ is shown for different values of the field in the case (I) $h_y=h_z$: from left to right are the data for $h_z=-0.1J, 0J, 0.3J, 0.5J, 0.7J$. The lines serve as a guide to the eye.

$$\varphi(\Delta E)=\frac{1}{1+\exp\left(\frac{\Delta E}{k_BT}\right)}, \tag{2}$$

relating two spin configurations of the system $\{\sigma\}\Rightarrow\{\sigma'\}$ which differ only by the exchange of two nearest-neighbor spins. ΔE is the corresponding change in the energy of the system, i.e.,

$$\Delta E=H(\{\sigma'\})-H(\{\sigma\}). \tag{3}$$

Most of the simulations are performed for a system of size L^3, $L=15u$, where u is the lattice constant. Larger system sizes are also considered in few cases. The density was kept fixed at $\rho=0.4$ during the simulations. The temperature was set to $T=3.8J/k_B$, sufficiently below the critical temperature of the 3D Ising model, $T_c^{3D}\approx 4.51J/k_B$ [14,15] so that the correlation length ξ is small (of the order of one lattice spacing $\xi\sim u$, see, e.g. [16,17,18]). The results are usually averaged over $N_{\text{ens}}\geqslant 500$ runs. Typical Monte Carlo simulation lasted $(1.6-2)\times 10^5$ Monte Carlo steps (MCS) per site.

III. RESULTS

A. Homogeneous substrates

To determine whether the equilibrium state is reached, we first studied the case $h_y=h_z$ where at equilibrium one should get a completely symmetric shape of the drop with respect to the plane of symmetry $z=y$. We kept track also of the total energy $E(t)$ of the system and the bulk phase magnetization $m_b(t)$ versus time t. But the slowest relaxing quantity in the system is the shape of the drop. It relaxes slower than the first layer radius $R_1(t)$ of the drop in contact with the substrate. In the cases where $h_y\neq h_z$, to ensure that indeed the equilibrium state is reached, we also performed some additional runs starting from a completely random initial configuration with $\rho=0.4$ and the same boundary conditions arriving at the same final equilibrium state. The two cases, (I) $h_y=h_z$ and (II) $h_y\neq h_z$, simply correspond to two different geometries studied.

The averaged distribution of the magnetization along the y axis in every layer z at equilibrium, $\bar{m}(z,y)=\langle m(z,y)\rangle$, is defined in the following way:

$$\bar{m}(z,y)=\frac{1}{N_{\text{ens}}}\sum_{k=1}^{N_{\text{ens}}} m_k(z,y)=\frac{1}{N_{\text{ens}}}\sum_{k=1}^{N_{\text{ens}}}\left(\frac{1}{L_x}\sum_{x=1}^{L_x}\sigma_k(z,y,x)\right). \tag{4}$$

The magnetization profiles $\bar{m}_1(y)$ of the first layer $(z=1)$ at equilibrium for different fields h_z in the case (I) $h_z=h_y$ are shown in Fig. 2. From there the first layer radius of the drop at equilibrium R_1 was determined as the point at which $\bar{m}_1(R_1)=0$. In the same way we proceeded to determine the projection of the shape of the drop in the (z,y) plane. Depending on the substrate field h_z one gets, as expected, a complete range of behavior, see Fig. 3, i.e., ranging from a nonwetting at $h_z=-J$ in the case $h_y=0.7J$ fixed and varying h_z [case (II)], through partial wetting, to a complete wetting regime. While in the case $h_y=h_z$, if one applies high negative

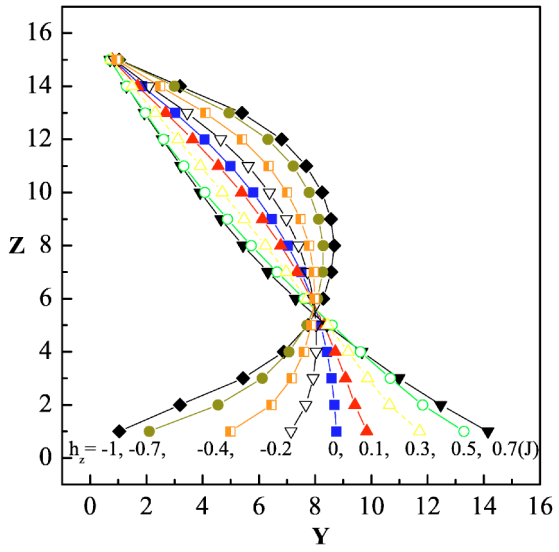

FIG. 3. (Color online) The averaged profiles of the drop in the (z,y) plane at equilibrium ($T=3.8J/k_B$, $\rho=0.4$) are shown for case (II): $h_y=0.7J$ fixed and different surface fields $h_z \in [-1J, 0.7J]$. The lines connecting the data serve as a guide to the eye.

field the drop starts separating in the corner, e.g. at $h_z \approx -0.4J$, and at $h_z=-J$ the drop is at the center of the system, see Fig. 4. In the partial wetting regime studied here in the interval $h_z \in (0, 0.7J)$ there is not qualitative difference in the quantities of interest in the two cases, see, e.g., Fig. 5.

The reduced first layer radius $r_1=R_1/L$ is a linear function of the surface field h_z in a wide interval of values of h_z as can be seen from Fig. 4. The deviation at high field $h_z > 0.6J$ is

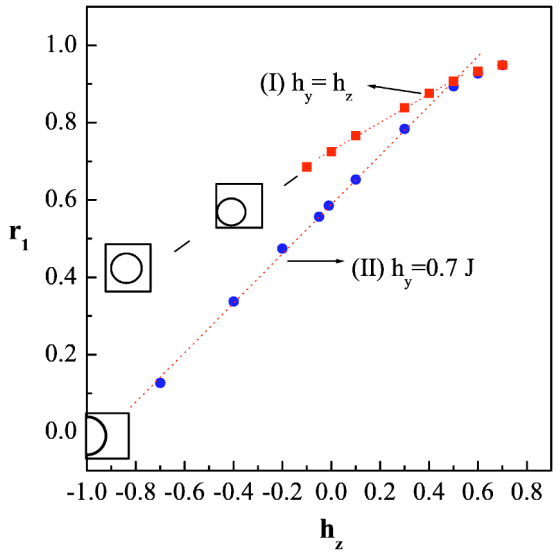

FIG. 4. (Color online) The reduced first layer radius $r_1=R_1/L$ versus the surface field h_z in (J units) is shown at $T=3.8J/k_B$: in the case (I) $h_y=h_z$, solid squares, and in the case (II) $h_y=0.7J$ fixed and varying h_z, solid circles. The dotted lines are the corresponding linear fits. The inserts show schematically the forming of the drop in the middle of the system at $h_z=-1J$ in the $h_y=h_z$ case and the forming of a half-drop at the wall $y=0$ when $h_y=0.7J$ is fixed and h_z varies.

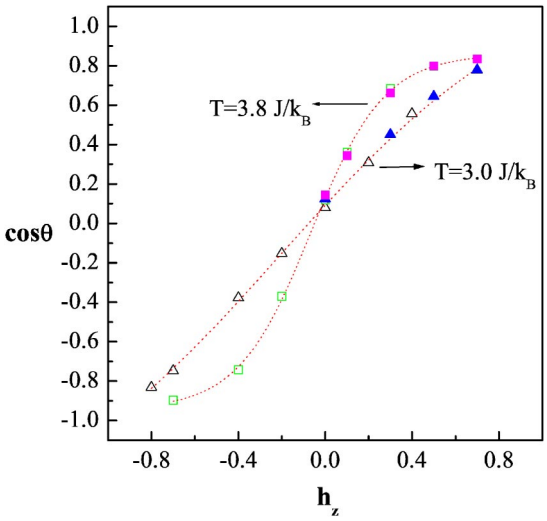

FIG. 5. (Color online) The cosine of the contact angle $\cos\theta$ versus the surface field h_z (in J units) is shown: at $T=3.8J/k_B$ in the case (I) $h_y=h_z$, solid squares, and in the case (II) $h_y=0.7J$ fixed and varying h_z, open squares, and at $T=3.0J/k_B$ in the case (I) $h_y=h_z$, solid up triangles, and in the case (II) $h_y=0.7J$ fixed and varying h_z, open up triangles. The dotted lines are the fits with the sigmoidal (Boltzmann) function.

due to approaching the wetting field h_w at this temperature. The wetting temperature for the semi-infinite 3D Ising model is estimated to be $T_w^{3D} \approx 3.8J/k_B$ for $h_z=0.64J$ using the results in [19,20,21]. Indeed, at a lower temperature, e.g., at $T=3.0J/k_B$, one can see a linear behavior practically in the whole interval $h_z \in (0, \ldots, 0.7J)$, since at $T=3.0J/k_B$ the wetting field is $h_w \approx 0.86J$.

Though in a lattice system, like the IM, one should rather use the Wulff construction [22] to get the proper contact angle, one can still try to define local contact angle in the simplest possible way and attempt to study how it behaves as a function of the surface field h_z and of the temperature T. Following that approach we define the "contact angle" θ using the obtained shape of the drop, shown in Fig. 3, by fitting the first few points, closest to the substrate, by a parabola and taking the derivative at $z=2$. At $T=3.8J/k_B$ the cosine of the so defined contact angle as a function of the surface field h_z, displayed in Fig. 5, is well fitted by a sigmoidal (Boltzmann) function. Note, that the $\cos\theta$ is practically the same function for the two considered cases: (I) $h_y=h_z$, where the case $h_y=h_z$ is well defined (i.e. for $h_z \geqslant -0.1J$, and (II) $h_y=0.7J$ is fixed and h_z varies.

We get also that the contact angle θ is a linearly increasing function of the temperature T in the interval $k_BT/J \in [3.0, 4.2]$ in the case $h_y=h_z$ below the wetting temperature as can be seen from Fig. 6. The little arrows denote the approximate positions of T_w for the corresponding field h_z. This result is in general agreement with the experimental results in [23].

B. Substrate with single-site impurities

We have studied the effect on the final state of the drop produced by single-site impurities with different concentra-

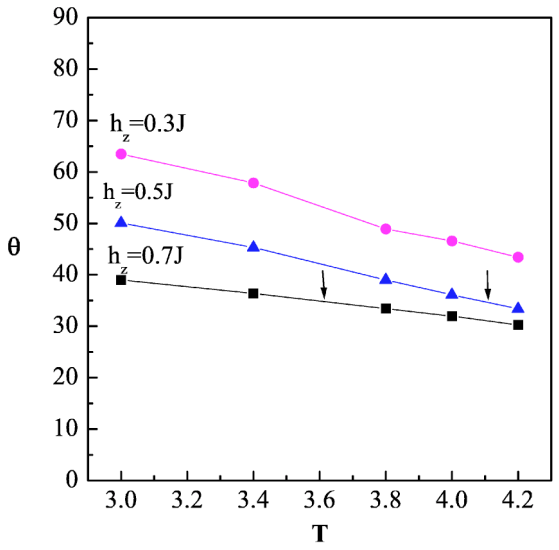

FIG. 6. (Color online) The contact angle θ (in degrees) versus the temperature T (in J/k_B units) is shown in the case (I) $h_y=h_z$ for different values of the surface field h_z: $h_z=0.3J$, solid circles, $h_z=0.5J$, solid up triangles, and $h_z=0.7J$, solid squares. The lines serve as a guide to the eye. The little arrows denote the approximate position of the wetting temperature at the corresponding field $T_w(h)$.

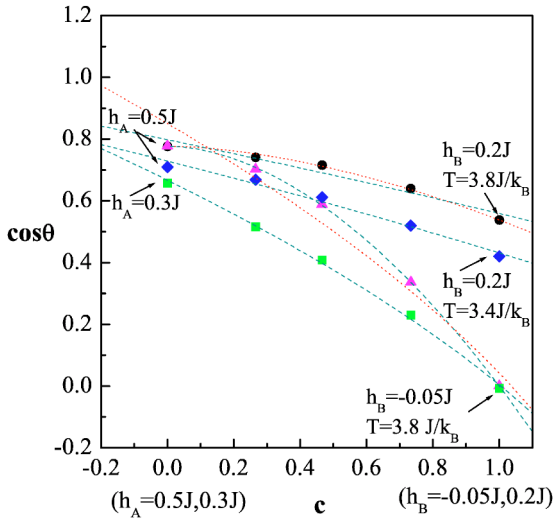

FIG. 7. (Color online) The cosine of the contact angle $\cos\theta$ versus the concentration c of single-site impurities is shown for several combinations of the pure substrates ($h_z=h_A$ at $c=0$ and $h_z=h_B$ at $c=1$): in the case $h_y=0.3J$ and $h_A=0.3J$, $h_B=-0.05J$ (solid squares), $h_y=0.5J$ and $h_A=0.5J$, $h_B=-0.05J$ (solid up triangles), at $T=3.8J/k_B$; and also for $h_y=0.5J$ and $h_A=0.5J$, $h_B=0.2J$ at two different temperatures: at $T=3.8J/k_B$ (solid circles), and at $T=3.4J/k_B$ (solid diamonds). The dashed lines are the best fits with Israelachvili's equation. The dotted lines are the corresponding best fits with the power function $f(c)=a_1-a_2c^p$.

tions. The point impurities are assigned a surface field h_B different from the rest of the substrate, h_A, and are regularly distributed in every layer $\{y,z=0\}$, $y=1,\ldots,L$. The shape of the drop and the contact angle change significantly with the concentration. Starting with a concave shape and $\theta\approx 39°$, when the field $h_y=0.5J$ is fixed and the surface field is $h_z=h_A=0.5J$ corresponding to 0% concentration of impurities, one obtains a convex shape and $\theta\approx 90°$, when the surface field is $h_z=h_B=-0.05J$ corresponding to 100% concentration of impurities.

In Fig. 7 we have presented the results we obtained for the cosine of the contact angle as a function of the concentration c of point impurities for several combinations of the surface fields of the pure substrates at two temperatures.

For the 2D IM [24] using numerical simulations it was shown that Cassie's law [25] is compatible with the data. We have tested our data for heterogeneous surfaces against Cassie's equation:

$$\cos\theta(c) = c\cos\theta_B + (1-c)\cos\theta_A \tag{5}$$

and Israelachvili's equation [26]:

$$[1+\cos\theta(c)]^2 = c(1+\cos\theta_B)^2 + (1-c)(1+\cos\theta_A)^2, \tag{6}$$

where $\cos\theta_A$ and $\cos\theta_B$ are the cosines of the contact angle on the pure substrates and $\cos\theta(c)$ is the cosine of the effective contact angle on the heterogeneous substrate at concentration c of the impurities with a surface field h_B. We find here that at low temperatures and low surface fields there is a good agreement of our data with Cassie's and Israelachvili's equations. The agreement with Israelachvili's equation is slightly better—see, e.g., the results for $h_A=0.3J$, $h_B=-0.5J$ at $T=3.8\ J/k_B$ and $h_A=0.5J$, $h_B=0.2J$ at ($T=3.4\ J/k_B$) in Fig. 7. At high temperatures and high fields there is a deviation from the linear law in concentration. The concentration dependence is then described by a power function, i.e., $\cos\theta(c)=a_1-a_2c^p$, where a_1 and a_2 are related to the cosines of the contact angles of the pure substrates: $a_1=\cos\theta_A$, and $a_2=\cos\theta_A-\cos\theta_B$. Thus for the considered substrates with point impurities one has

$$\cos\theta(c) = \cos\theta_A + (\cos\theta_B - \cos\theta_A)c^p. \tag{7}$$

If $p=1$ this reduces to the familiar Cassie's equation.

We find that $p\approx 1.83$ for $h_y=0.5J$ and $h_A=0.5J$, $h_B=-0.05J$. The error of the fitting is $\chi^2\leqslant 5\times 10^{-5}$. The power p decreases with decreasing h_A (while h_B is kept fixed) and with the temperature T. That is the deviation from the linear behavior is stronger at higher temperatures and for stronger interactions with the substrate.

The advancing interface in the first ($z=1$) layer, i.e., the position of the triple line as function of time, was also recorded. The way in which the impurities affect the contact line motion is well illustrated in Fig. 8. The impurities change the velocity of the contact line, in this particular example they temporarily trap the contact line and slow down its motion. Even when the contact line overcomes the impurities it is still deformed and the deformation of the contact line in the final equilibrium state depends on the strength, size and the position of the impurities.

C. Time evolution of the drop

We find that there exists certain interval of values of the surface field h_z, e.g., $h_z\in(0.1J,0.6J)$ at $T=3.8J/k_B$, such that

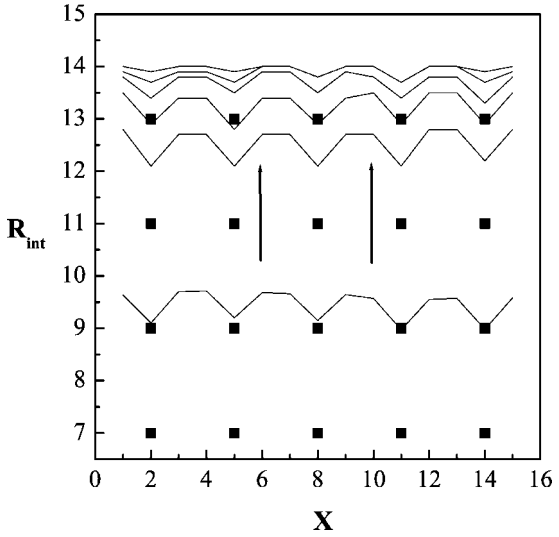

FIG. 8. The averaged position of the interface R_{int} in the (x,y) plane as function of x (both in lattice spacings) at the first layer $z=1$ on a substrate with impurities is shown at several successive values of the time. The black squares show the place of the impurities and the arrows denote the direction of spreading.

the time behavior of the first layer radius $R_1(t)$ is well described by an exponential decay function, i.e., $R_1(t)=y_0-A\exp(-t/\tau_r)$, where $y_0=R_{eq}$ is the equilibrium value of the base radius and τ_r is a characteristic relaxation exponent. Typical simulation runs for the base radius of the spreading drop at $T=3.8J/k_B$ are shown in Fig. 9. Within the same interval of surface fields h_z, the time evolution of the cosine of the contact angle, shown in Fig. 10, is also well described by an exponential decay function but with different relaxation exponent $\tau_{\cos\theta}$.

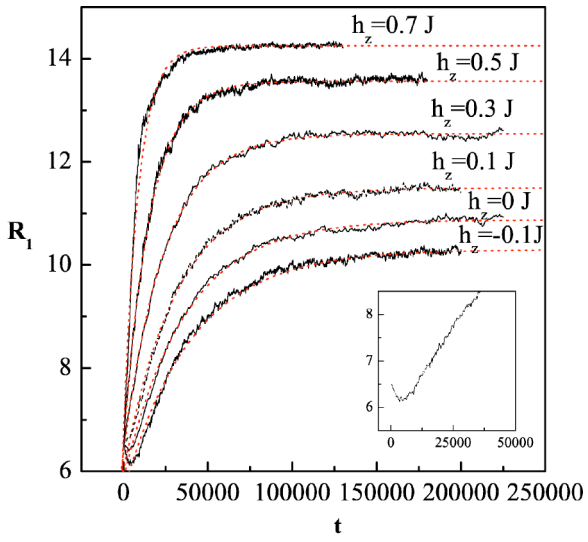

FIG. 9. (Color online) The time (in MCS per site) evolution of the base radius $R_1(t)$ (in lattice spacings) at $T=3.8J/k_B$ in the case (I) $h_y=h_z$ for several values of the surface field h_z, from bottom to top: $h_z=-0.1J,0.0J,0.1J,0.3J,0.5J,0.7J$. The dotted lines are the best exponential decay fits. The inset shows the time behavior for small times of the base radius at $h_z=-0.1J$.

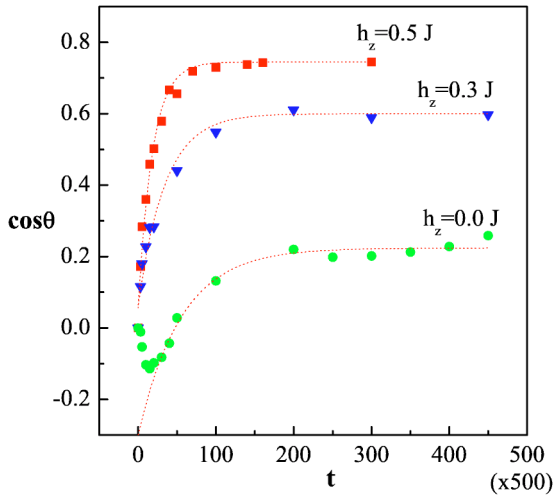

FIG. 10. (Color online) The time (in MCS per site) evolution of the cosine of the contact angle $\cos\theta(t)$ at $T=3.8J/k_B$ in the case (I) $h_y=h_z$ for several values of the surface field h_z, from bottom to top: $h_z=0.0J$, solid circles; $h_z=0.3J$, solid down triangles; $h_z=0.5J$, solid squares. The dotted lines are the best exponential decay fits.

As can be seen from Fig. 9, at fixed temperature T when the field h_z increases, the time behavior of $R_1(t)$ changes and the quality of the fit with an exponential decay function gets worse. At $h_z=0.7J$ for $T=3.8J/k_B$ the system is actually in the wetting regime, at least the semi-infinite system. If one further increases the system size, at $h_z=0.7J$ and $T=3.8J/k_B$, one finds that the time behavior of the first layer radius changes to an exponential growth function.

For low and negative surface fields, i.e., for $h_z\leqslant 0.1J$, two regimes are observed in the time behavior of $R_1(t)$. At first $R_1(t)$ decreases with t (see Fig. 9, $h_z=-0.1J,0J$) and then there is a time interval where again its behavior is well described by an exponential decay function. The same holds for the time behavior of the cosine of the contact angle. For low values of the field it is difficult to determine τ_r and $\tau_{\cos\theta}$ correctly. For the temperatures and positive surface fields considered we find that the base radius relaxes slower than the cosine of the contact angle, i.e., $\tau_{\cos\theta}<\tau_r$. For example we find that typical relaxation times (in MCS per site) are as follows: for $h_z=0.5J$, $\tau_{\cos\theta}=9120$ and $\tau_r=15684$; for $h_z=0.3J$, $\tau_{\cos\theta}=17500$ and $\tau_r=24287$; while for $h_z=0J$ we have $\tau_{\cos\theta}=72785$ and $\tau_r=36338$.

From the exponential decay fits of the base radius $R_1(t)$ and $\cos\theta$ it follows that for times smaller than $\tau_{\cos\theta}$ the interface velocity $v=dR_1/dt$ is proportional to the driving force $F_{dr}\propto\cos\theta_0-\cos\theta(t)$, i.e., that the following equation holds for R_1:

$$\frac{dR_1}{dt}=b(T,h_z)[\cos\theta_0-\cos\theta(t)], \tag{8}$$

where $b(T,h_z)$ is a coefficient of proportionality and θ_0 is the equilibrium contact angle. Let us recall that the molecular kinetic model by Blake *et al.* [27], in its linear form, relates the base radius and the cosine of the contact angle θ at time t through the following equation:

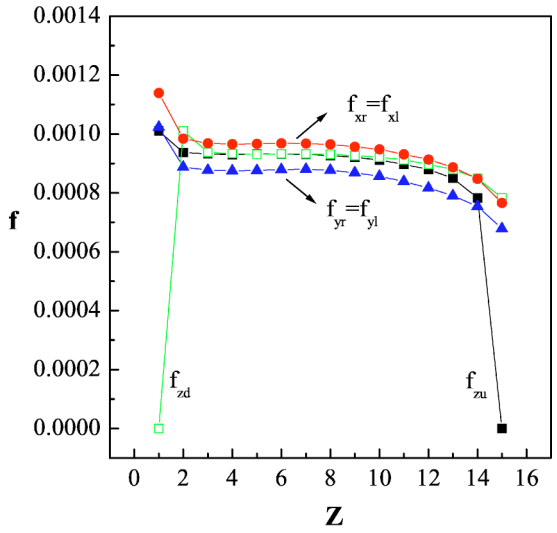

FIG. 11. (Color online) The jump frequency [in (MCS per site)$^{-1}$] distributions in different layers are displayed in the equilibrium state at $T=3.8J/k_B$ for $h_z=0.5J$ in the case (I) $h_y=h_z$: f_{zd} (empty squares), f_{zu} (solid squares), $f_{yr}\equiv f_{yl}$ (solid up triangles), and $f_{xr}\equiv f_{xl}$ (solid circles). The lines serve as a guide to the eye.

$$\frac{dR_1}{dt}=\frac{\gamma}{\zeta}(\cos\theta_0-\cos\theta), \tag{9}$$

where ζ is the friction coefficient and γ is the interface tension. So the Blake and Haynes molecular kinetic theory gives a valid description of the initial stages of spreading of the 3D IM drop. Comparing the two equations it follows that the coefficient of proportionality $b(T,h_z)=\gamma/\zeta$. This relation can be used in principle to determine the friction coefficient ζ if the interface tension γ is known.

We studied also the mobility of the particles in the different layers of the drop. The frequency for jumps at the z layer in the positive (right) y direction (this is the direction of the spreading of the drop) is defined as the average of the ratio of the number of particles which have moved in the right y direction at the z layer in one MCS per site over the total number of particles in the system, i.e.,

$$f_{yr}(z)=\langle N_{yr}(z)/N_{part}\rangle. \tag{10}$$

In a similar way are defined the frequencies for jumps in the z (up and down) and in the x (right and left) directions. Typical distributions of the frequencies for jumps in the different layers at equilibrium are shown in Fig. 11. One can see that in the bulk the different frequencies for jumps change slightly and the values they have are very close. There are significant differences at the end-layers and particularly in the first layer, all the frequencies are higher, except for $f_{zd}(z=1)$ which is zero of course. The frequencies for jumps in the y direction (right and left) are slightly lower than in z and x directions due to the existence of the interface. At the end layers, i.e., $z>11$ all the frequencies are slightly lower due to the fact that there are less particles than in the bulk. For high interaction with the substrate, e.g., $h_z=0.5J$, the total mobility of the particles in the first layer is lower than

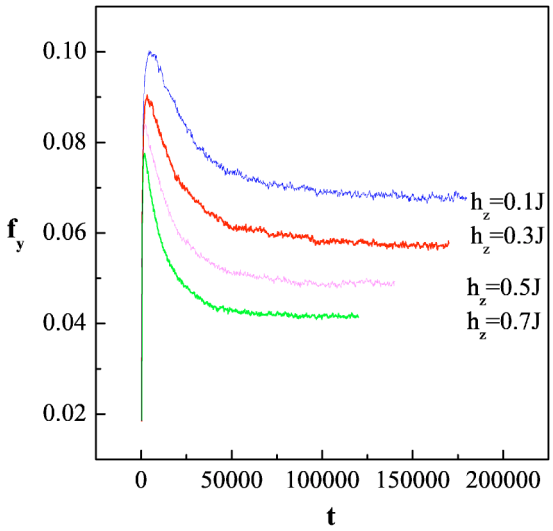

FIG. 12. (Color online) The time (in MCS per site) dependence is shown of the frequency $f_y(z=1)$ [in (MCS per site)$^{-1}$] for jumps in the y direction in the first layer, defined as the ratio of the realized jumps in the y direction over the attempted jumps in the y direction in the first layer in one MCS per site at $T=3.8J/k_B$. The four different lines are for different values of the surface field h_z of the substrate in the case (I) $h_y=h_z$, from top to bottom: $h_z=0.1J, 0.3J, 0.5J, 0.7J$.

in the bulk, while for lower fields, e.g., $h_z=0.2J, 0.3J$, it is the opposite. We find also, see Fig. 12, that the frequencies for jumps in the first layer decrease when the surface field increases, i.e., the interactions with the substrate get stronger, in agreement with the MD simulations by de Ruijter *et al.* [28].

We have studied and plotted in Fig. 13 the temperature dependence of the frequency for jumps in the spreading direction f_{yr}. As can be seen the temperature dependence is well fitted by the following function:

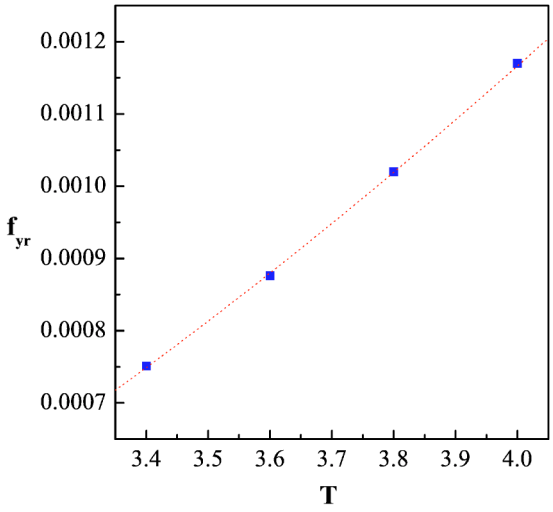

FIG. 13. (Color online) The frequency for jumps in the spreading direction f_{yr} [in (MCS per site)$^{-1}$] versus the temperature T (in J/k_B units) is shown at $h_z=0.5J$ in the case (I) $h_y=h_z$. The dotted line is the best fit by $f(T)=p_1T\exp(-p_2/T)$, where $p_1=0.00143$, $p_2=6.36$.

$$f_{yr}(T) = 0.00143\, T \exp(-6.36/T). \quad (11)$$

This temperature dependence is in agreement with the molecular kinetic theory of liquids by Eyring *et al.* [29] according to which the equilibrium frequency of displacements K_0 is related to the molar activation free energy ΔG_w through

$$K_0 = \frac{k_B T}{2\pi\hbar} \exp(-\Delta G_w / N_A k_B T), \quad (12)$$

where N_A is the Avogadro's number and $\hbar$ is the Planck constant. This expression for the frequency of displacements enters into the Blake and Haynes theory of spreading.

IV. CONCLUSIONS

The MC simulations of the 3D IM on heterogeneous substrates show that at low temperatures and low surface fields there is a good agreement of the data with Cassie's and Israelachvili's equations, the agreement with Israelachvili's equation being slightly better. At high temperatures and high surface fieds there is a deviation from the Cassie's and Israelachvili's equations. Then the concentration dependence of the cosine of the contact angle is well described by a power function.

The obtained temperature dependence of the contact angle on homogeneous substrates is in a qualitative agreement with the experimental results in [23].

We find that the time behaviors of the first layer radius and the cosine of the local contact angle in certain interval of values of the surface h_z field within the partial wetting regime are well described by exponential decay functions. From this it follows that the interface velocity is proportional to the driving force:

$$\frac{dR_1}{dt} = b(T, h_z)[\cos\theta_0 - \cos\theta(t)] \quad (13)$$

for times smaller than relaxation time $\tau_{\cos\theta}$. Thus the Blake and Haynes molecular kinetic theory gives a valid description of the initial stages of spreading of the 3D IM drop.

We find also that the temperature dependence of the equilibrium frequency for jumps in the spreading direction, f_{yr}, is consistent with the temperature dependence given by the Blake and Haynes theory.

ACKNOWLEDGMENTS

N.C.P. gratefully acknowledges the hospitality of the Centre de Recherche en Modélisation Moléculaire and financial support from FNRS which made this collaboration possible.

[1] K. Binder and D. Heermann, *Monte Carlo Simulation in Statistical Physics* (Springer-Verlag, Heidelberg, 1997).
[2] E. Cheng and C. Ebner, Phys. Rev. B **47**, 13808 (1993).
[3] S. Tan, Colloids Surf., A **148**, 223 (1999).
[4] J. D. Coninck, Colloids Surf., A **80**, 131 (1993).
[5] J. D. Coninck, N. Fraysse, M. P. Valignat, and A. M. Cazabat, Langmuir **9**, 1906 (1993).
[6] A. M. Cazabat, J. D. Coninck, S. Hoorelbeke, M. P. Valignat, and S. Villette, Phys. Rev. E **49**, 4149 (1994).
[7] F. Heslot, A. M. Cazabat, P. Levinson, and N. Fraysse, Phys. Rev. Lett. **65**, 599 (1990).
[8] F. Heslot, N. Fraysse, and A. M. Cazabat, Nature (London) **338**, 640 (1989).
[9] J. D. Coninck, S. Hoorelbeke, M. P. Valignat, and A. M. Cazabat, Phys. Rev. E **48**, 4549 (1993).
[10] J. D. Coninck, U. D'Ortona, J. Koplik, and J. R. Banavar, Phys. Rev. Lett. **74**, 928 (1995).
[11] K. Kawasaki, Phys. Rev. **145**, 224 (1966).
[12] K. Kawasaki, in *Phase Transitions and Critical Phenomena*, edited by C. Domb and M. S. Green (Academic, New York, 1972), Vol. 2.
[13] K. Binder, D. P. Landau, and A. M. Ferrenberg, Phys. Rev. Lett. **74**, 298 (1995).
[14] C. F. Baillie, R. Gupta, K. A. Hawick, and G. S. Pawley, Phys. Rev. B **45**, 10438 (1992).
[15] A. Ferrenberg and D. P. Landau, Phys. Rev. B **44**, 5081 (1991).
[16] H. B. Tarko and M. E. Fisher, Phys. Rev. B **11**, 1217 (1975).
[17] K. Binder, D. P. Landau, and D. M. Kroll, Phys. Rev. Lett. **56**, 2272 (1986).
[18] M. Hasenbusch and K. Pinn, Physica A **192**, 342 (1993).
[19] K. Binder, D. P. Landau, and S. Wansleben, Physica A **40**, 6971 (1989).
[20] K. Binder and D. P. Landau, Phys. Rev. B **37**, 1745 (1988).
[21] K. Binder and D. P. Landau, Phys. Rev. B **46**, 4844 (1992).
[22] G. Wulff, Z. Kristallogr. Mineral. **34**, 449 (1901).
[23] M. de Ruijter, P. Kölsch, M. Voué, J. D. Coninck, and J. P. Rabe, Colloids Surf., A **144**, 235 (1998).
[24] D. Urban, K. Topolski, and J. D. Coninck, Phys. Rev. Lett. **76**, 4388 (1996).
[25] A. B. D. Cassie, Discuss. Faraday Soc. **3**, 11 (1948).
[26] J. Israelachvili and M. Gee, Langmuir **5**, 288 (1989).
[27] T. D. Blake and J. M. Haynes, J. Colloid Interface Sci. **30**, 421 (1969).
[28] M. J. de Ruijter, T. D. Blake, and J. D. Coninck, Langmuir **15**, 7836 (1999).
[29] S. Gladstone, K. J. Laidler, and H. J. Eyring, *The Theory of Rate Processes* (McGraw-Hill, New York, 1941).